SPIRAL SECTOR MAGNETS

D. W. KERST

Midwestern Universities Research Association (USA) *

Field magnets with alternating gradient focusing can be made by the introduction of a spiral spatial ripple into the magnetic field. Without the use of poles excessively close to the median plane the type of variation of magnetic field which is most readily obtainable is sinusoidal. To obtain a field which would subject the particles to alternating focusing forces, the median plane field originally conceived was of the form

$$B_{zo} = B_0 (r/r_0)^k \left[1 + f \sin\left(\frac{r-r_0}{\lambda} - N\theta\right)\right].$$

In order that the field scale, however, in such a way that the essential features of its effect on particles at all radii be the same, we use the form

$$B_{zo} = B_0 (r/r_0)^k \left[1 + f \sin\left(\frac{ln(r/r_0)}{w} - N\theta\right)\right],$$

with w constant.

From these expressions it is seen that N is the number of spiralling ridges passed over by a particle in going around the machine once in the θ direction. f is the fractional flutter in the magnetic field due to the ridges. Finally, if the radial width of the annulus is small in comparison to the outer radius, r_0, $\lambda = 2\pi\lambda \doteq 2\pi r_0 w$ is substantially the radial separation of the ridges. The exponent k is taken to be positive.

The equations of motion.

If one undertakes to write the linear terms in the differential equations characterizing the departure of the particle from a reference circle of radius $r_1 = p/eB_0 (r_0/r_1)^k$, one obtains substantially the following, where $x \equiv (r - r_1)/r_1$ and $y \equiv z/r_1$.

$$x'' + \left[1 + k + \frac{f}{w}\cos N\theta\right] x \doteq f \sin N\theta$$

$$y'' - \left[k + \frac{f}{w}\cos N\theta\right] y \doteq 0.$$

These equations suggest alternate gradient focusing of the type characterized by the Mathieu differential equation, but the presence of the forcing term on the right hand side of the equation for the x-motion indicates that a forced oscillation will be expected and will be given approximately by

$$x = -\frac{f}{N^2 - (k+1)} \sin N\theta.$$

Because of the presence of this forced motion one realizes that not only will the nonlinear terms in the differential equations be large but that a noticeable influence upon the betatron oscillation wavelength can result.

It is appropriate, therefore, to perform an expansion about a more suitable reference curve by writing

$$v = x + \frac{f}{N^2 - (k+1)} \sin N\theta.$$

In this way one obtains equations of which the most significant terms appear below:

$$v'' - \left[k + 1 - \tfrac{1}{2}\frac{f^2/w^2}{N^2 - (k+1)} + \frac{f}{w}\cos N\theta + \tfrac{1}{2}\frac{f^2/w^2}{N^2 - (k+1)}\cos 2N\theta\right] v = 0$$

$$y'' - \left[k - \tfrac{1}{2}\frac{f^2/w^2}{N^2 - (k+1)} - \frac{f}{w}\cos N\theta + \tfrac{1}{2}\frac{f^2/w^2}{N^2 - (k+1)}\cos 2N\theta\right] y = 0$$

* Assisted by the National Science Foundation and the Office of Naval Research.

Solution of the equations of motion.

The solutions of equations of this type can be obtained numerically and their characteristics also obtained by variational methods. It is of interest, however, to note some general approximate conclusions which may be reached by application of the smooth approximation technique. By this latter technique, if the relatively small contributions from the terms involving cos 2N0 be neglected and if k + 1 is ignored in comparison to N^2, one finds that the general character of the motion is approximately represented by

$$v'' + (k + 1)\, v = 0$$

$$y'' + \left(\frac{f^2}{w^2N^2} - k\right) y = 0,$$

The overall effect of the field-flutter drops out of the equation for radial motion leaving the radial focusing essentially accounted for by the r^k field dependence. Axial focusing, however, can also be attained if the term $f^2/(w^2/N^2)$ is sufficiently large to dominate k.

In this smooth approximation the number of betatron wavelengths around the machine, for the radial and axial oscillations respectively, will be given by

$$\nu_r = \sqrt{k + 1}$$

$$\nu_z = \sqrt{\frac{f^2}{w^2N^2} - k}$$

A somewhat more extensive analytical investigation has been made along the foregoing lines and without use of the smooth approximation leading to results which, for small amplitude motion, appear to be in satisfactory agreement with information available from digital computer solutions of the exact differential equation for the motion. Fig. 1 graphically exhibits the phase changes, σ_r and σ_z, per sector as functions of k/N^2 and f/WN^2.

It appears possible to see qualitatively why, when the scalloped character of the equilibrium orbit is included, the constants of the oscillations are influenced in the sense in which they are. The curvature of the orbit is smaller as it passes through the high field over the ridges than it is as it passes through the lower field between the ridges. The particle passes through regions of alternately positive and negative field gradients. The longer path in the negative gradient regions due to the scallop helps the vertical focusing at the expense of the already strong radial focusing.

Modification of solution for separated spiral sectors.

The final approximate equations given above can be applied to spiral sector magnets in which the field in the median plane is not strictly sinusoidal. In this case, the only reinterpretation of the symbols is that for f one should substitute the effective value:

$$f = (\sqrt{2}/\bar{H}) \left[\frac{1}{S_0} \int_0^{SO} (H - \bar{H})^2 \, dS\right]^{\frac{1}{2}}$$

where $\bar{H}$ is the mean field along the path of the orbit, S; and S_0 is the length of the equilibrium orbit in one sector. In other words, f is the $\sqrt{2}$ times the root mean square deviation from the mean field divided by the mean field. We are interested in applying this to a magnet design described here which is composed of separate slanting sectors which the orbit crosses at a small angle. The field shape in the orbital plane is zero between sectors and rises to its full value within the magnet gap. In case the field free region has an abrupt edge and the same length as the region containing the field, $f = \sqrt{2}$. Another way to solve the linear equation for this type of accelerator is by the transfer matrix method. The parameters are for an accelerator with a magnetic field having a distribution in the orbital plane shown in fig. 2. This field shape is accomplished by winding the ridges with separate coils so that only the space in the gap between ridges has magnetic field. In this case the flutter, f, is equal to 1.28. This value of the flutter is sufficiently high that it allows the angle that the ridges make with the orbit to be about 8.5°. Fig. 3 shows the dimensions of the ridges for this case.

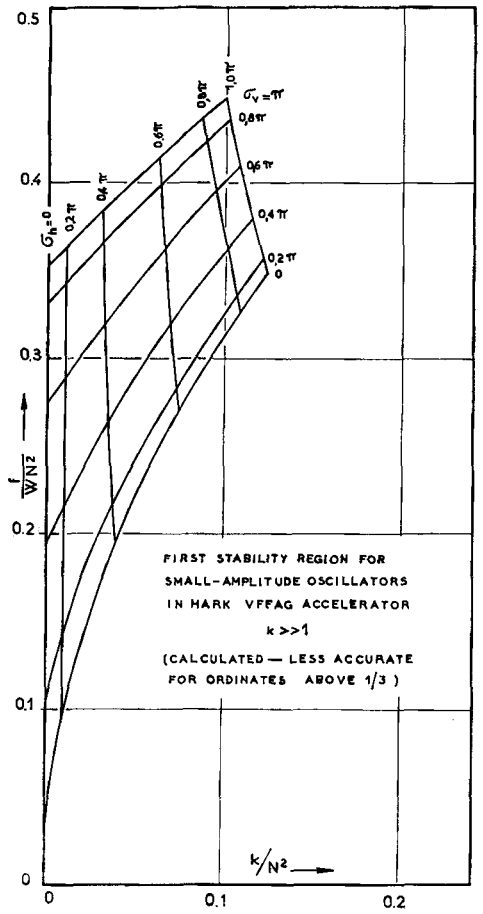

Fig. 1.

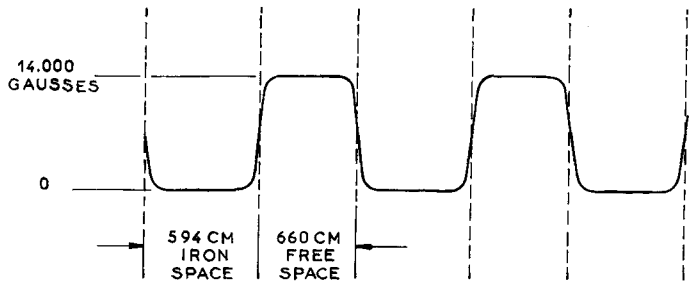

Fig. 2. Circumferential field distribution at 7,560 cm. radius with 22 cm. gap.

We choose the following parameters:

Energy of accelerator		— 15 Bev
Field within sector		— 14,000 gausses
	k	= 82.5
Mean orbit radius		— 7,560 cm.
5 Mev radius		— 7,154 cm.
Number of sectors		= 38
Radial separation of ridges		= 174 cm.
ν_r Number of radial betatron oscillations around the machine		= 10.8
	σ_r	= .57
	ν_z	= 4.85
	σ_z	= .255
Gap at injection radius		= 22 cm.
Gap at high energy radius		= 15 cm.

Although this accelerator has an average field of only 7,000 gausses and consequently a larger circumference than spiral sector accelerators with f = .25, it has many attractive features. For example:

1. The sectors are all isolated and can be wound separately with wire as shown in fig. 4. The backwinding across the pole face which provides the radial change of magnetic field is accomplished in the same way that the coils were wound at Purdue for the Michigan radial sector model.

2. The open spaces between sectors allow strengthening and supporting of the vacuum system.

3. These spaces provide field free regions which amount to straight sections which are necessary for the insertion of targets.

4. Another feature is that the large average angle between the ridge and the orbit, 8.5°, eliminates much of the nonlinear character of the orbital motion observed in cases where the flutter, f, is only .25. The nonlinear radial amplitude stability limit for this type of accelerator is probably as great as 70 centimeters, whereas the amplitude of the largest oscillation desired in the aperture will probably be of the order of eight centimeters.

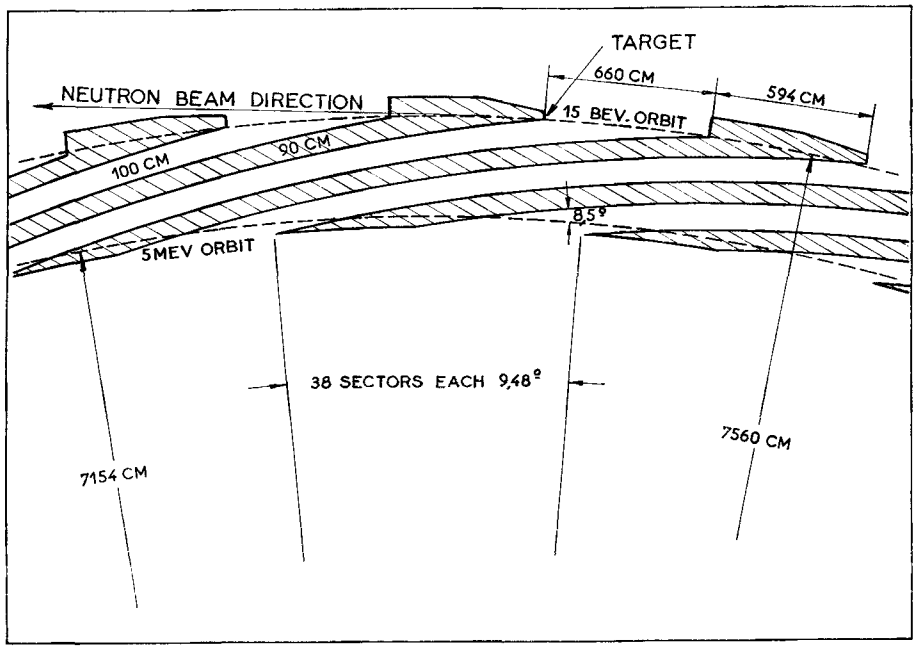

Fig. 3. Spiral sector dimensions.

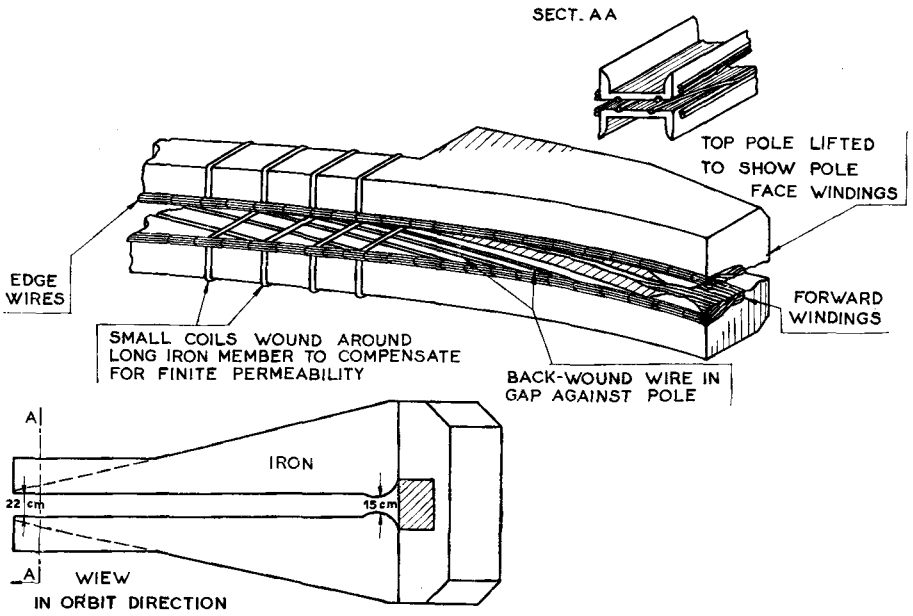

Fig. 4. View of sector.

5. Since the angle is as large as 8.5°, it is not unreasonable to lengthen the field free region greatly by merely moving the isolated sectors farther apart at certain azimuths. This provides access to the beam for experimental purposes, and it does not destroy the scaling properties of the accelerator, which would be destroyed if a radial cut were made in the magnet.

6. The return yokes for the magnetic field occupy, only about 50 percent of the circumference of the magnet thereby leaving large gaps allowing a target to be placed so that the straightforward neutron beam from it passes easily out between the return yokes. Extracted charged particle beams can be brought out through these same spaces.

7. By fine control of the angle which the separated sectors make with the orbit the wave length of the vertical oscillation can be adjusted after the accelerator is erected.

All the above features can be considered advantages over the more compressed type of radial sector accelerator which has its ridges attached to a continuous magnetic pole and which has a flutter, g, equal to .25. The details of the latter type machine and its problems of construction are shown later. The disadvantages of the separated spiral sector arrangement are:

1. That it takes somewhat more iron, since its circumference and aperture are larger.

2. The long ridges will need some external support.

3. The long ridges need additional distributed ampere-turns just to drive flux along them.

The following figures on the iron, power, and copper are derived for the case of the magnet with the iron cross section of the ridge tapered linearly from the high field to the low field end, which means high flux density iron is only at the high field end. The copper is used at a current density of 1,200 amperes per square inch, which will allow air cooling with ducts where the coil is deep, although there may be some small portions which need water cooling.

Iron weight	11,400 tons/accelerator (300 tons per ridge)
Copper	800 tons/accelerator (21 tons per ridge)
Power	5 megawatts/accelerator (130 kilowatts per ridge)

In case the variation of the magnetic field in the median plane is senusoidal we find that the equipotential surfaces established by the iron become deeply creviced if the magnetic gap is too large. We can estimate how large a gap is possible without the crevices going to infinity. This calculation is included here and it has frequently been taken as a criterion for determining the limiting gap size in spiral sector accelerators. However, it is improper to consider this calculation as giving a limiting gap size since it is merely necessary to deviate from the sinusoidal field variation to achieve bigger flutters and larger gaps.

We examined the problem for a two-dimensional case which approximates the spiral ridge case. We take $B = B_0 \gamma^k (1 + f \sin x/\lambda)$ with the magnetic potential for the case of $k = 0$ as $V = B_0 \{Y + f\lambda \sin x/\lambda \cdot \sinh Y/\lambda\}$.

We want to calculate the maximum gap between opposing pole ridge tops, G, for different values of the fractional field variation, f, in the median plane. This maximum G is the separation between ridge tops for the limiting magnetic equipotential which develops an infinite crevice between ridges.

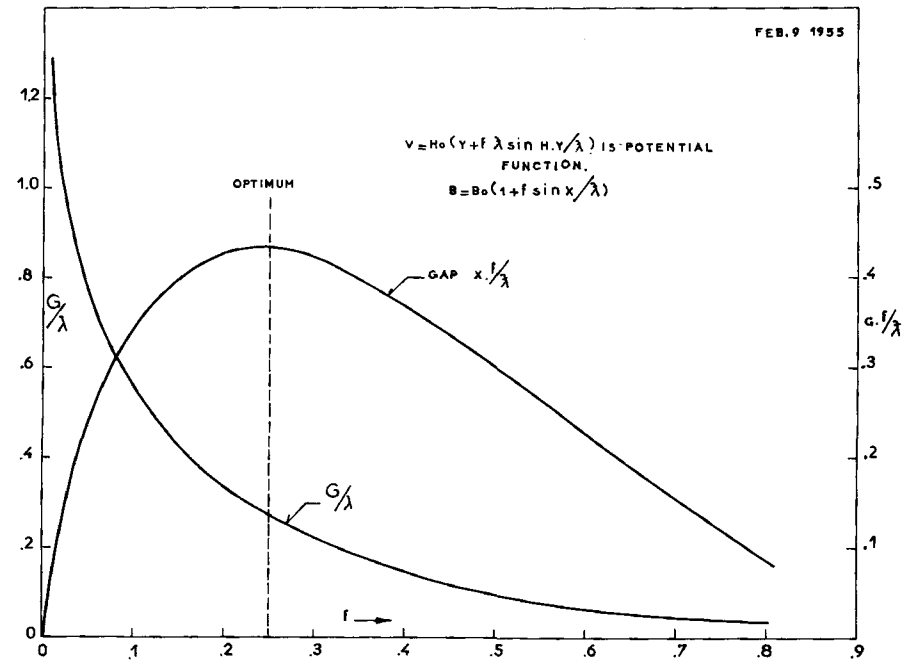

Fig. 5. Plot of minimum gap in spiral ridged poles (ridges spaced λ) as a function of the flutter F.

The crevices occur where $dV/dY = 0$ or

$$0 = 1 + f \sin x/\lambda \cdot \cosh (Y_\infty/\lambda)$$

and the value of x/λ at crevices is $x/\lambda = -\pi/2$. Thus $1/f = \cosh (Y_\infty/\lambda)$. For this equipotential

$$V_\infty = B_0 \{\lambda \cosh^{-1} 1/f = \lambda f\sqrt{(1/f^2) - 1)}\} \quad .$$

On this same equipotential surface $Y_{min} = G/2$ occurs at $\sin x/\lambda = +1$ and it satisfies

$$V_\infty = B_0 \{Y_{min} + f\lambda \sin H (Y_{min}/\lambda)\}$$

equating

$$\frac{Y_{min}}{\lambda} + f \sin H \left(\frac{Y_{min}}{\lambda}\right) = \cos H^{-1} \frac{1}{f} - \sqrt{(1 + f)(1 - f)}.$$

If we now impose the condition that the smooth approximation $\nu^2_z = \dfrac{f^2 r^2}{\lambda^2 N^2} = 2A.G.$ be a constant, then since in cases where $k \neq 0$ N is already chosen by radial motion considerations, we are imposing the condition f/λ = constant. This is also requiring that $dB/dx \Big|_{max}$ ≡ constant in the orbital plane for different parameters tried.

The graphs (fig. 5) show $G/\lambda = 2\,Y_{min}/\lambda\,(2\,\pi)$ determined by the transcendental equation above and $G\,f/\lambda$ which is proportional to the maximum gap attainable for f/λ = constant, ν_z = constant, or $\left(\dfrac{r\ dH}{H\ dr}\right)_{Peak}$ = constant.

The curves show that $f = 1/4$ gives about the maximum gap if one is designing for a fixed ν_z, but only 10% of

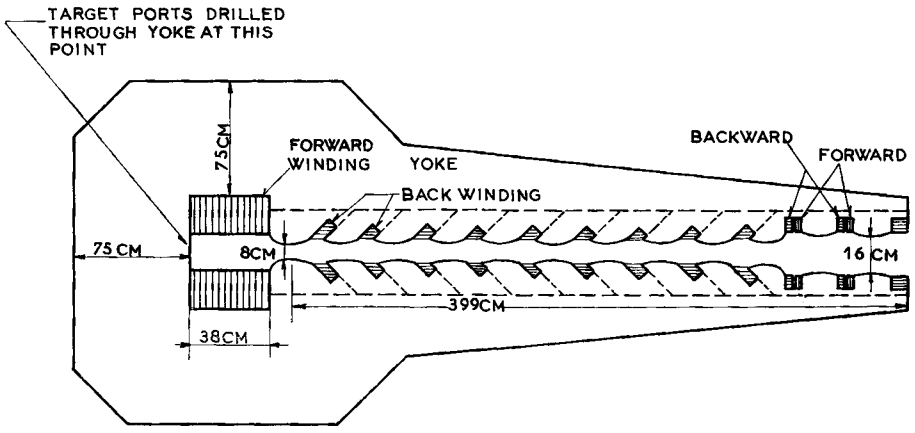

Fig. 6. 25 Bev spiral sector FFAG magnet.

Fig. 7a. Spiral sector model section.

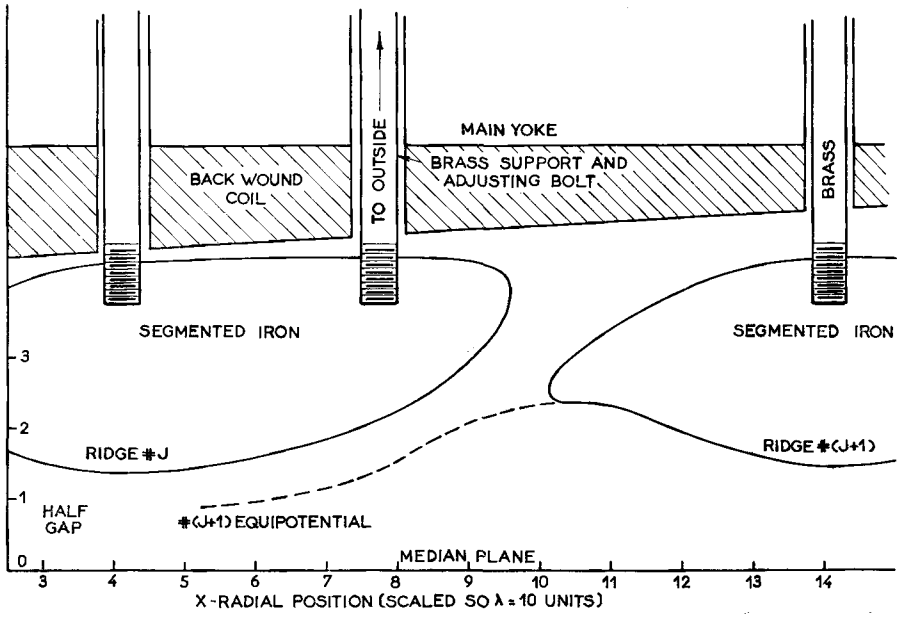

Fig. 7. Method of floating equipotentials.

the gap is lost if f = .35 or .15 is used. The biggest usable value of G/λ is .28 which is a good design rule. This result is very closely the same as that given by the Illiac for the solution to the Cauchy problem with $k \sim 150$, that is for $B = B_0 (r/r_0)^k (1 + f \sin x/\lambda)$ in the orbital plane. We next describe a different style of spiral sector accelerator, which is given here to exhibit some other solutions to several design problems, for the case of a small flutter f = .25. The pole pieces are large forgings with machined spiral ridges, as shown in fig. 6 or the ridges may be supported bars of segmented iron as shown in fig. 7. Such floating equipotentials are also shown in the photograph of a spiral sector model section (fig. 7a). There is difficulty inserting radial cuts for straight sections in spiral sector accelerators, because these straight sections disturb the periodicity differently at different radii. Studies have been undertaken to determine the best way to design these straight sections, and there are indications that they may be as long as 70 cm., which would be sufficient for the insertion of RF accelerating cavities and targets. Although it is desirable to have longer straight sections, it is not yet certain that this can be accomplished. Consequently, beam extraction and access ports may have to be put through the return yoke at some azimuths. This is shown in fig. 8.

One possible shape of the iron poles has been determined by the digital computer. Fig. 9 shows the equipotentials with an idealized copper distribution to maintain the gap essentially the same at all radii. Fig. 10 indicates how the copper can be imbedded in a slot at the high field portion of the pole where the amount of copper is large. Fig. 11 illustrates a method of opening the gap at the injection radius so that there is more space at injection. This is accomplished by forward and backward currents in the current slot. Such extra currents are not objectionable at the low field rim of the magnet, because very little current is required there. Fig. 12 illustrates how the currents can be brought back across the ridges at three points

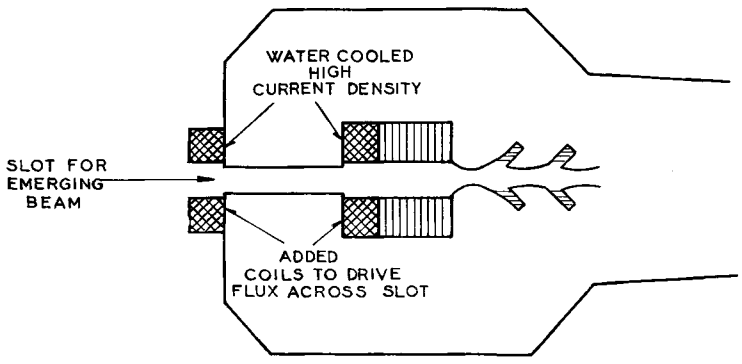

Fig. 8. Sector with beam removal slot.

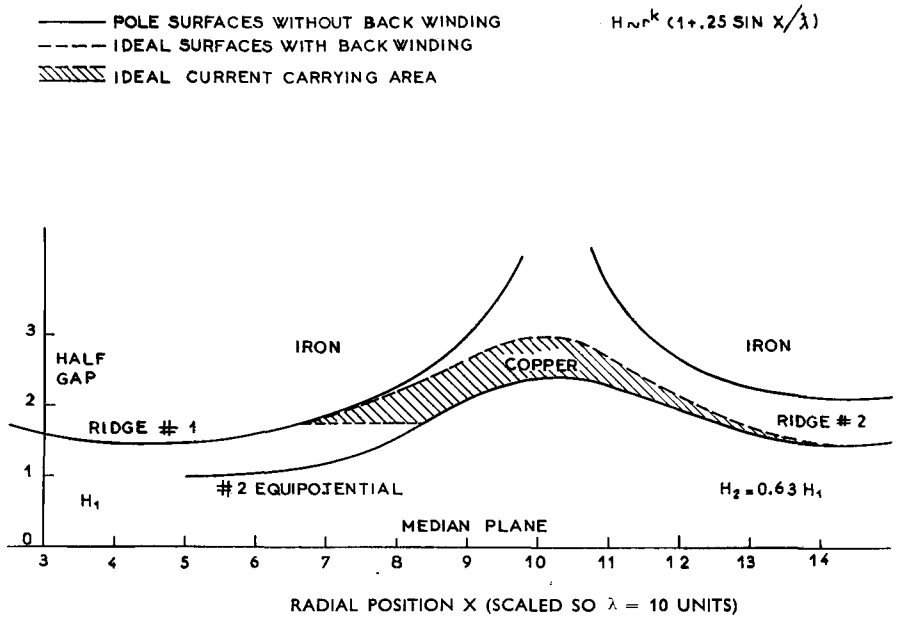

Fig. 9. Digital computer equipotentials.

in a sector so that the gap along a ridge does not have to open very much at the low field end.

In these structures, the vacuum would probably have to enclose the backwound coil imbedded in the pole.

Typical parameters for a structure giving 25 Bev are listed below. Two points should be borne in mind: First, although the figures given show the low energy orbit to be 4 Mev at injection, this should not be taken as indicating that that is the best choice of injection energy. We have many injectors from which to choose—linear accelerators or cyclotrons from 10 to 50 Mev or the Van de Graaf accelerators for 4 to 10 Mev. The second point is that the parameters given below will almost certainly need adjustment when the complete effects of straight sections and magnet imperfections and stability limits for the amplitude are fully determined. It has been shown by digital computer studies that it is essential to avoid $\sigma_x = = (2/3)\pi$. It is expected that amplitude limits to stability near to $\sigma_x = (2/3)\,\pi$ can be influenced by design. The stability sought should be greater than the aperture available between the poles of the magnet.

Final energy	25 Bev
Injection energy	5 Mev
Final radius	6,172 cm. = r_0

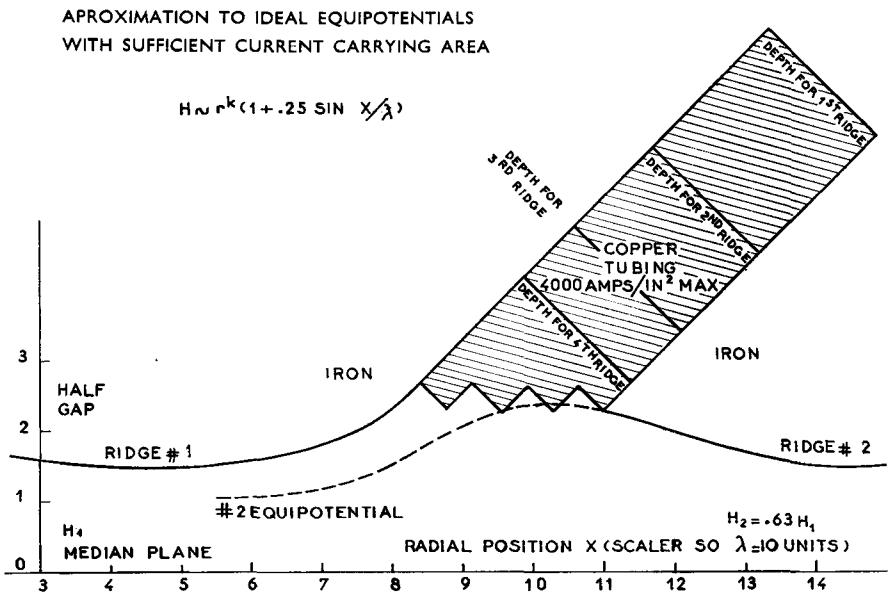

Fig. 10. Digital computer equipotentials.

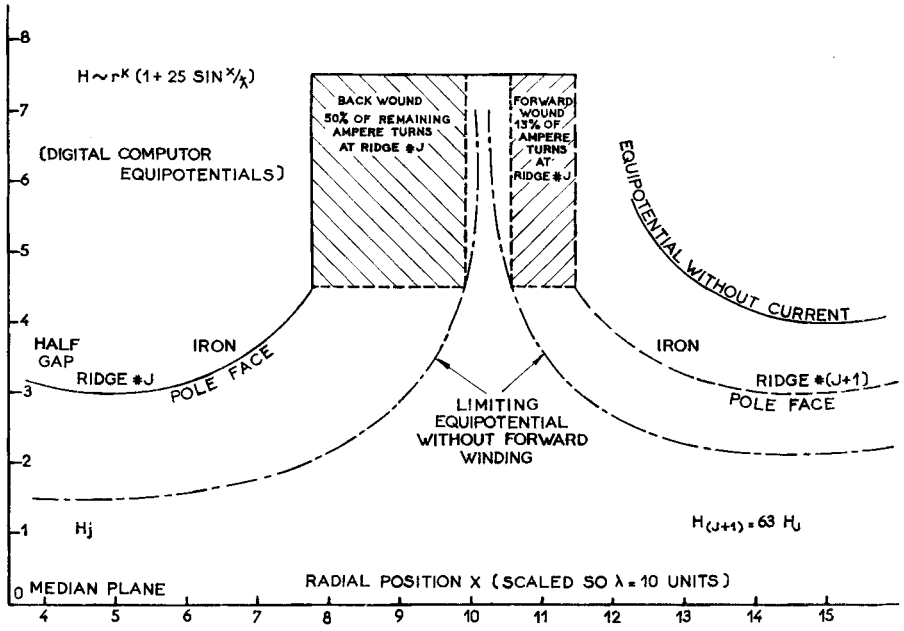

Fig. 11. Backward and forward slot windings to allow gap to open by twice limiting equipotential gap.

Injection radius	5,767 cm. = r_i
Aperture	405 cm. = $r_0 - r_i$
k	82.5
$\bar{H}_0$	14,000 gausses average field
f	.25
w	1/1,320
radial separation of ridges	29.4 cm.
σ_x	.615 π
σ_z	.25 π
ν_x	10.15 radial betatron oscillations in a circumference
ν_z	4.15 axial betatron oscillations in a circumference
N	33 sectors
Weight of iron	20,600 tons
Weight of copper	382 tons
Power comsumption	4,900 kW for magnet

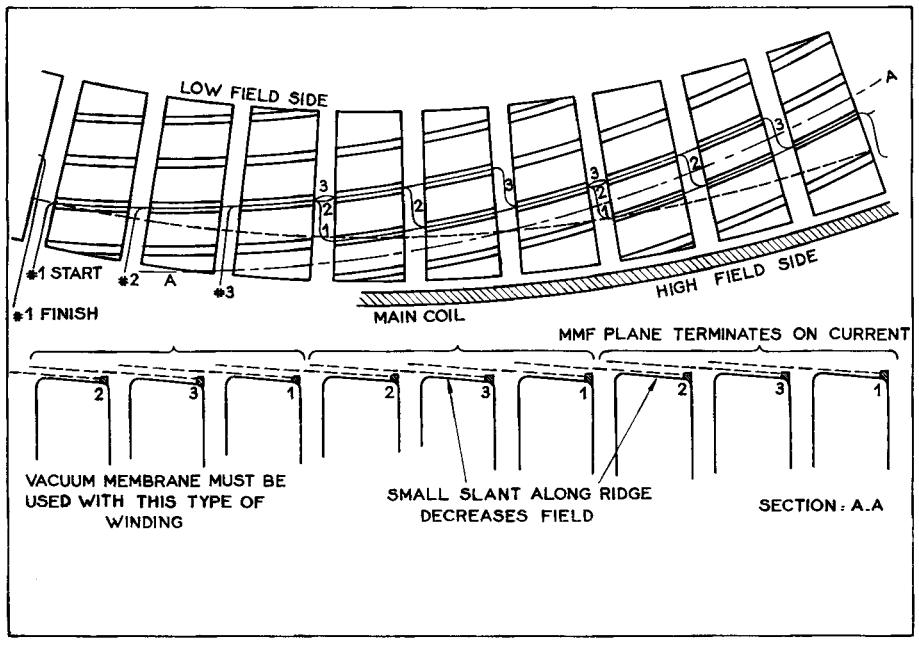

Fig. 12. Schematic ridge crossing.

	Weight of Copper	*Electrical Power*
Main coil	= 247.5 tons	1,560 kilowatts
First slot	= 28.5 tons	1,930 kilowatts
Second slots	= 28.5 tons	743 kilowatts
Third slots	= 28.5 tons	284 kilowatts
Remainder	= 49.5 tons	383 kilowatts

One of the severe problems of the spiral sector accelerator is the production of a large flutter, f, without an uncomfortably small gap between the poles. In the example given in this section, a flutter of only .25 was used. This flutter can be increased several fold by shaping the ridges. This increase allows the radial separation of ridges to increase by the same factor, since to keep the same betatron wave length f (ridge separation) must be constant. With the larger ridge separation, the gap can be opened proportionately, which is a desirable result, particularly at the low energy radius. A disadvantage of increasing the flutter is that the average magnetic field is lowered, and, consequently, the circumference for a given energy is increased.

Remarks

I will indicate some developments which were not included in the material in the preprint.

Numerous tests have been made on the influence of misalignment of portions of a spiral sector accelerator. These tests were made with a digital computer. The motion in the spiral sector accelerator is strongly influenced by non-linear forces. In general a stability limit on the amplitude of the motion is reached when the tune σ changes with amplitude due to non-linear effects until it reached the value of $2\pi/3$ or $2\pi/4$. When either of these frequencies for the motion is reached, because of the variation of σ of amplitude, then for practical purposes the coordinate suffers a wide excursion and hits the wall of the tube of the vacuum vessel. Of the two values for σ, $2\pi/3$ appears to be the more serious in the spiral sector accelerator. $2\pi/4$ is less harmless and $2\pi/5$ does not seem to be very serious.

When misalignments are tested by the computer the stability limit is observed to shrink in magnitude even though the zero amplitude σ is retuned to the value for an ideal machine. One case of the spiral sector magnet has been examined in considerable detail in this respect, and in the course of these investigations improvements in structures have been evolved.

Studies by T. Ohkawa, L. J. Laslett, A. M, Sessler and J. N. Snyder have produced a better understanding of some of the problems involved. The tune of the radial motion, σ_r is practically independent of the variation of the flutter of the magnetic field. However the tune of the axial motion, σ_z, is strongly dependent on the magnitude of the flutter, f. We know that the magnitude of the flutter increased with distance from the median plane. Consequently one can make estimates of the amplitude of axial motion sufficient to increase the flutter to the point where σ_z reaches $2\pi/3$ or $2\pi/4$. These estimates give rough agreement with the stability limits determined by the digital computer for axial motion. The rate of increase of flutter with distance from the median plane is greater for fields containing harmonics higher than the fundamental sector frequency. However for flat poles and separated ridges, each with its own set of coils, the harmonic content can distort the field shape strongly from the fundamental without serious decrease of the axial amplitude stability limit. Introducing higher harmonics has a beneficial effect since it increases the effective flutter, and when the effective flutter is increased, it is possible to turn the ridges in a more radial direction, thus separating them more widely and allowing the gap between poles to be increased. One can go fairly far in increasing the flutter by the addition of harmonics before the axial stability limit is depressed substantially and the consequent allowable enlargement of the ridge separation permits an increased axial stability limit up to the point where the harmonic content becomes too high. With less than this optimum harmonic content one can actually have the gap between poles considerably greater for the same tune but the size of the axial stability limit actually becomes smaller and hence much of the space between the poles cannot be used by orbits. For example with $^1/_2$ of the circumference iron it is possible to have flutters of 1.15 at the optimum and to have the total gap about $^1/_4$ of the ridge separation of the radial direction with the axial stability limit filling this gap to the extent of about 70 per cent to 90 per cent. At smaller flutters larger gaps can be used, still giving the same tune if the radial ridge separation is decreased, but the absolute value of the axial stability limit decreases.

The stability limit for radial motion is also increased if the flutter can be increased. A simple reason for this is that the ridges may be directed more radially and the quadratic forces are thereby decreased. In general the limiting amplitudes for spiral sector non-linear motion are proportional to w^2/f, where w is proportional to the radial separation of the sectors and f is the effective flutter. Since the tune depends on w/f, then for a given tune the higher the flutter the larger the stability limit appears to be.

High flutter machines require a large circumference but reasonable compromise can be made. Approximate methods of treating an exponential growth in axial motion have been developed following a suggestion by W. Walkinshaw. W. Walkinshaw examined the case $2\sigma_z = \sigma_r$ and treated it by inserting the approximate radial motion of finite amplitude in the axial differential equation. Periodicity created in the axial differential equation by the insertion of the radial motion causes instability if the amplitude of the radial motion exceeds a certain value. Under these circumstances the axial motion increases

exponentially with time at least when its amplitude is somewhat below the axial stability limit. Other cases as $\sigma_z + 2\,\sigma_r = 2\pi$, $2\,\sigma_z + 2\,\sigma_r = 2\,\pi$ and $2\,\sigma_z = 2\,\sigma_r$ have been treated by L. J. Laslett and A. M. Sessler. These treatments are used to tell us how wide danger lines on the working point diagram are for radial motions of different amplitudes. This work has proven very important in the choice of parameters for spiral sector models.